

Design Feature

ZHENG RUIQING | Senior Design Engineer ZHANG GUOHAO | Design Engineer ZHANG ZHIHAO | Design Engineer

Guangdong University of Technology, School of Information Engineering, Guangzhou 510006, PRC; +86-13450222131, e-mail: 460071860@qq.com

EM Analysis Guides WLAN PA Design

This power amplifier module, which was designed with the help of EM simulation and analysis, is well-suited for WLAN applications from 4.9 to 5.9 GHz.

Power amplifiers (PAs) for wireless local-area networks (WLANs) in the industrial-scientific-medical (ISM) band at 2.4 GHz are enabling high-speed wireless data communications in a wide range of locations, including homes, offices, and airports. WLAN radios working at ISM frequencies have provided data-transmission speeds to 54 Mb/s, and this frequency band is becoming more and more crowded with the ever-growing number of users.

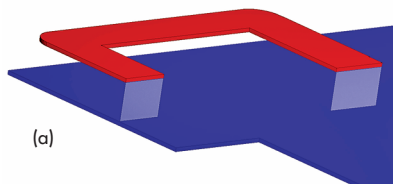
To avoid loss of bandwidth and bit rates at 2.4 GHz, the unlicensed national information infrastructure (UNII) band at 5 GHz provides an alternative frequency range for WLAN radios. This higher-frequency band features 12 non-overlapping chan-

nels and can support data transmissions at 10 times the rates possible at 2.4 GHz. In support of 5-GHz WLANs, a power amplifier module (PAM) was developed with the aid of electromagnetic (EM) analysis techniques and broadband matching theory. It provides better than 1 W of saturated output power from 4.9 to 5.9 GHz while operating on +3.3-V dc bias.

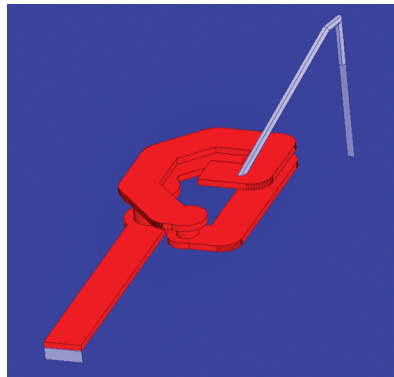
The IEEE has defined requirements for 5-GHz UNII-band WLANs by its IEEE 802.11ac standard.¹ For PAs, the standard poses challenging requirements for vector-error-magnitude (EVM) performance for all operating conditions and flat gain across the band.² At higher frequencies, implementing a PA that meets these requirements becomes difficult due to excessive

characteristic capacitance and inductance of the PA circuit elements. However, by using EM analysis and wideband impedance matching, a high-output PAM was developed for WLAN applications. The amplifier achieves better than +29-dBm output power at 1-dB compression from 4.9 to 5.9 GHz.

The PAM consists of two parts: an InGaP/GaAs heterojunction-bipolar-transistor (HBT) monolithic-microwave-integrated-circuit (MMIC) amplifier device and a high-frequency circuit laminate. The laminate was simulated by means of three-dimensional (3D) EM models and EM analysis techniques. In the analysis of the EM models of inductors on the laminate or capacitors in the InGaP/GaAs HBT MMIC, some parasitic parameters are extracted to create simple equivalent circuits for the design of the broadband matching network. The laminate's inductors consist of microstrip lines or bonding wires. Any parasitic capacitance from these

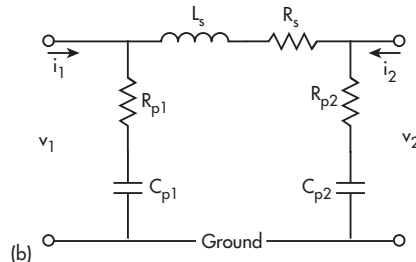
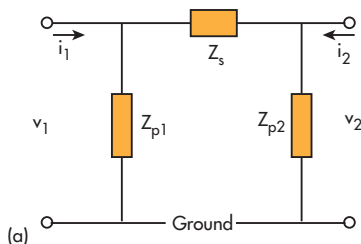


(a)

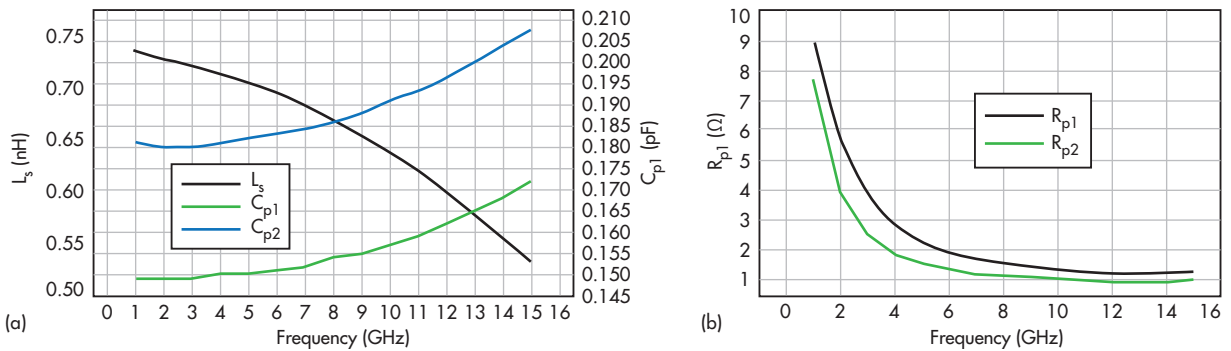


(b)

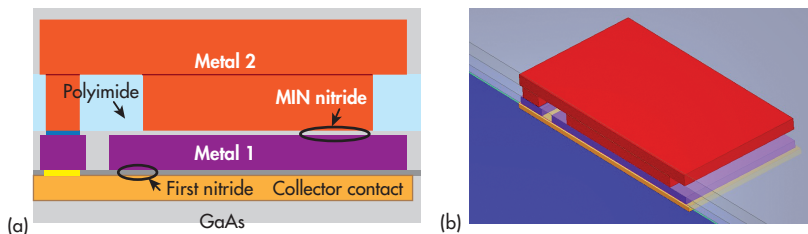
1. These images portray (a) the output impedance-matching inductor and (b) the power bias inductor on the laminate of the PAM.



2. These equivalent circuits represent (a) the inductors in Fig. 1(a), and (b) the equivalent-circuit parameters.



3. These curves show the dependence of the circuit parameters of Fig. 2(b) for (a) the effective inductance, L_s , and (b) resistances added by the parasitic capacitances.



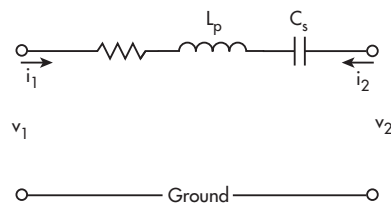
4. This is (a) cross-sectional view of a stacked capacitor and (b) an EM model of a stacked capacitor.

inductors will complicate the creation of an impedance matching network for the PAM, since this capacitance will be part of the matching network.

Figure 1 shows several 3D EM models—for the microstrip of an output matching network on the laminate in (a), as well as a bond wire and microstrip serving as the bias power inductance in (b). This microstrip transmission line serving as an inductor is different from an ideal inductor: It exhibits distributed capacitance between the transmission line and the ground. According to a differential model of the transmission line,³ an equivalent circuit was proposed to describe the parasitic characteristics of the inductor in Fig. 1(a); the parameters of this circuit can be extracted from EM simulation results. Equivalent circuits for Figs. 1(a) and (b) are shown in Figs. 2(a) and (b).

The inductor in Fig. 1(a) can be considered a two-port network. Using EM analysis, the network's S- and Y-parameters can be found over a wide frequency range. The parameters of the equivalent circuit in Fig. 2(b) also can be found through EM simulation.

The inductor in Fig. 1(a) can be regarded as a two-port network. Using the EM techniques described above, the S-parameters and Y-parameters of this network can be obtained over a wide frequency range. After the electromagnetic simulation, the parameters of the equivalent



5. This is an equivalent-circuit model for the stacked capacitor component in Fig. 4(b).

circuit in Fig. 2 (b)—which describe the frequency characteristic of the inductors—can be calculated from the Y parameters. According to the definition of Y-parameters, Eq. 1 can be obtained from Fig. 2(b), and the parameters in Fig. 2(b) can be calculated using Eqs. 1 and 2:

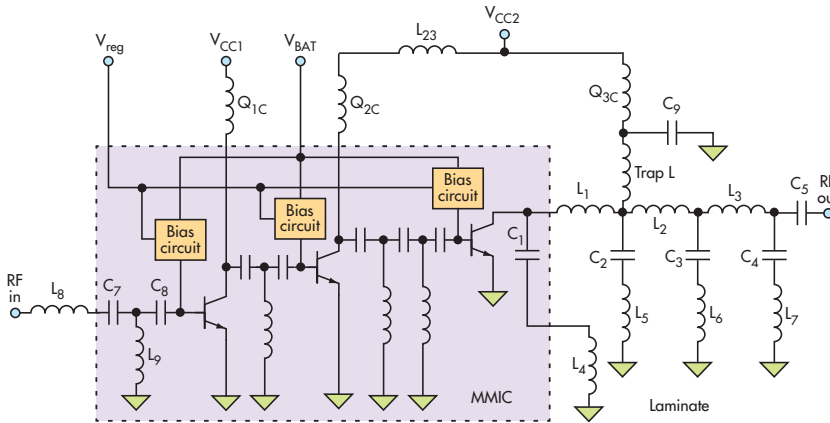
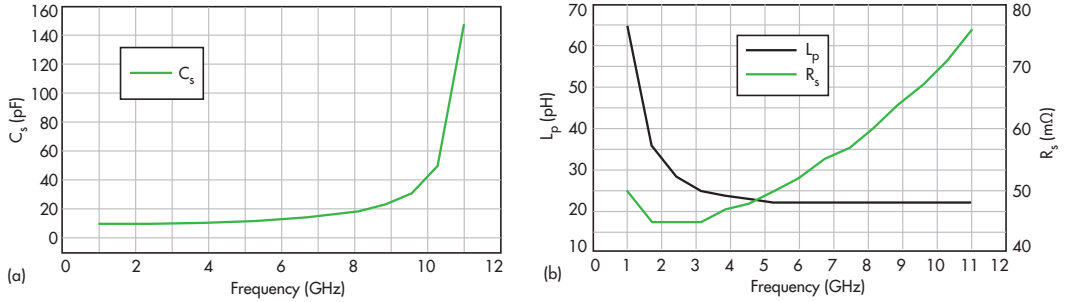
$$\begin{pmatrix} i_1 \\ i_2 \end{pmatrix} = \begin{pmatrix} Y_{11} & Y_{12} \\ Y_{21} & Y_{22} \end{pmatrix} \begin{pmatrix} v_1 \\ v_2 \end{pmatrix} \quad (1)$$

$$\begin{cases} Z_s = R_s + j\omega L_s = \frac{-2}{Y_{12} + Y_{21}} \\ Z_{p1} = R_{p1} + \frac{1}{j\omega C_{p1}} = \frac{1}{Y_{11} + Y_{12}} \\ Z_{p2} = R_{p2} + \frac{1}{j\omega C_{p2}} = \frac{1}{Y_{22} + Y_{21}} \end{cases} \quad (2)$$

The parameters in Fig. 2(b) for the inductor of Fig. 1(a) are shown from 1 to 15 GHz in Figs. 3(a) and (b). The effective inductance, L_s , decreases and the parasitic capacitances C_{p1} and C_{p2} increase with increasing frequency, which demonstrate that the frequency-dependent parasitic characteristics of inductors should be taken into account in the high-frequency range. The frequency-dependent parasitic characteristics of the power bias inductor in Fig. 1(b) also can be evaluated by the equivalent circuit in Fig. 2(b) following EM simulation.

The capacitor in the MMIC contributes to parasitic circuit elements in the PAM, too. Figure 4(a) shows a cross-sectional view of a stacked capacitor in the InGaP/GaAs HBT MMIC while Fig. 4(b) details its 3D EM model. At frequencies below 1 GHz, the parasitic capacitance of this capacitor can be ignored since the effective low-frequency capacitance of this circuit element is the same as its dc capacitance.

6. The plots show the dependence of the parameters in Fig. 5 of the capacitor in Fig. 4(b) from 1 to 11 GHz for (a) parasitic capacitance and (b) parasitic inductance.



7. This is a schematic circuit diagram representing the three-stage PA on the MMIC.

Based on EM simulation, the effective capacitance of this component increases in the UNII band. When the frequency exceeds the cutoff frequency of the capacitor, it works like an inductor. Figure 5 offers a simple equivalent circuit for the component in Fig. 4(b). Figure 6 shows the values for the circuit elements in this equivalent circuit from 1 to 11 GHz, based on EM simulation.

The dc capacitance of the capacitor component in Fig. 4(b) is 9 pF in this InGaP/GaAs HBT process, as confirmed by many designs below 1 GHz. The effective capacitance increases to about 11 pF at 5 GHz, according to the EM simulation results in Fig. 6(a). When the frequency increases to 8 GHz, the effective capacitance is about 30 pF since parasitic inductor L_s dominates at these higher frequencies. The value of L_s is almost the same from 4 to 11 GHz—about 20 pH.

In addition, the electrical connections to the capacitor of Fig. 4(b) add more parasitic inductance, making

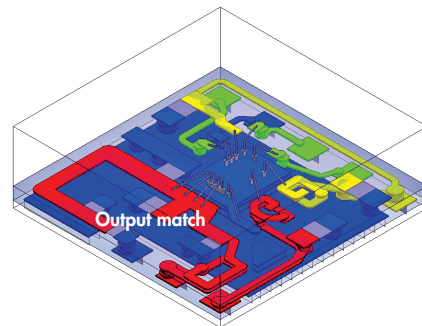
implementation of a matching network more difficult. However, this complexity can be solved through the use of EM analysis techniques. EM analysis makes it possible to account for the parasitic elements of the various passive components in the PAM's matching networks in great detail.

Figure 7 offers a schematic circuit diagram of a three-stage PA with inductors and capacitors not having high-frequency parasitic characteristics. Without the high-frequency parasitic characteristics, the schematic circuit diagram serves only as a guideline for the design parameters of each circuit element. More precise values can be obtained by means of EM analysis.

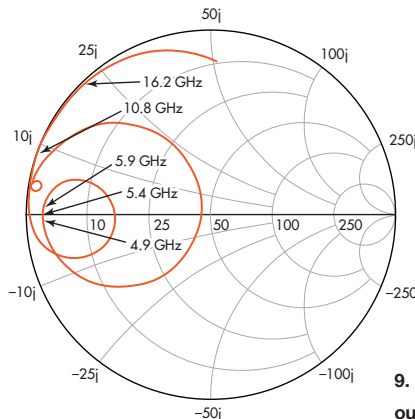
ACHIEVING THE AMPLIFIER

For 5-GHz WLAN use, the PAM was designed for operation from 4.9 to 5.9 GHz; its 1-GHz bandwidth will satisfy the requirements of the IEEE 802.11ac standard. To obtain low EVM, the output 1-dB compression point should be suitably high and the power gain should be flat, with minimal phase distortion to the 1-dB compression point. In this design, diode-based linearizing bias techniques⁴⁻⁶ have been used to improve linearity. With +3.3-V dc bias, the impedance of the output matching network must be low enough over the 1-GHz bandwidth to achieve saturated output power⁷ greater than 1 W. The output matching network is designed on the laminate according to Fig. 7 using EM techniques.

Figure 8 shows the EM model of the laminate without surface-mount capacitors, but with the addition of high-



8. The EM model represents the laminate without the surface-mount capacitors.

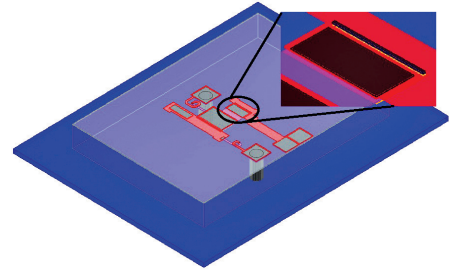


9. This is the EM-simulated impedance of the PA's output matching network.

frequency parasitic characteristics. *Figure 9* offers the EM-simulated impedance of the output matching network to the HBTs; the fundamental impedance is about 2.5Ω from 4.9 to 5.9 GHz, a low-enough value to attain the desired saturated output power for the PAM. The insertion loss of the output matching network is also less than 0.5 dB across the 1-GHz bandwidth.

The input matching network and interstage matching networks were designed on the MMIC to save area on the laminate.

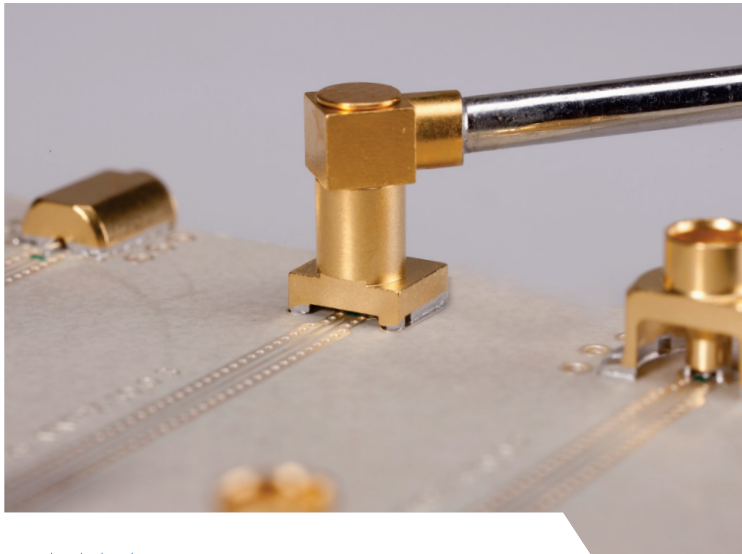
10. This is an EM model of the interstage matching network between the three-stage PA's middle and outer stages.



They consist of several L-type transformers to ensure a bandwidth of 1 GHz. The dc capacitances of the capacitors on the MMIC are less than the guidelines set in *Fig. 7*. In conjunction with the parasitic inductances produced in or around the actual capacitors, the effective capacitance in *Fig. 7* is obtained in the high-frequency range, according to EM analysis. With this design approach, the dc capacitance of the capacitors in the MMIC can be determined from EM simulation results.

Figure 10 shows an EM model of an interstage matching network between the PAM's middle and output stages in the MMIC; the simulated function is the same as the matching network in *Fig. 7*, but the dc capacitances of the capacitors in *Fig. 10* are less than the effective capacitances in *Fig. 7*.

Figure 11 shows the fabricated PAM. It consists of a PA MMIC, several surface-mount capacitors, and bond wires on a microwave laminate. The InGaP/GaAs HBT MMIC measures $1000 \times 700 \mu\text{m}$. The emitter area of the output stage is $4,800 \mu\text{m}^2$ and the emitter areas of the first- and second-stage HBTs are 960 and $480 \mu\text{m}^2$, respectively. The input matching network consists of two capacitors,

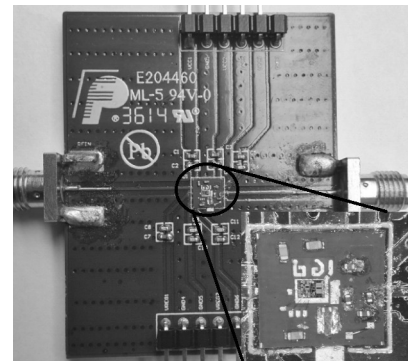


MMPX Superior signal integrity

The snap-on connector family HUBER+SUHNER MMPX is the most ideal coaxial-to-PCB system solution for operating frequencies up to 67 GHz. MMPX connectors feature excellent electrical performance and outstanding electrical stability at smallest mechanical dimensions. The broadband characteristics, the small size and the outstanding performance permit new solutions for applications in numerous markets such as high speed digital testing and radio frequency testing.

> www.hubersuhner.com

HUBER+SUHNER AG 9100 Herisau/Switzerland
HUBER+SUHNER INC. Charlotte NC 28273/USA



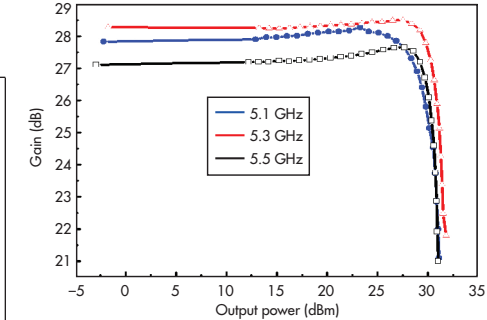
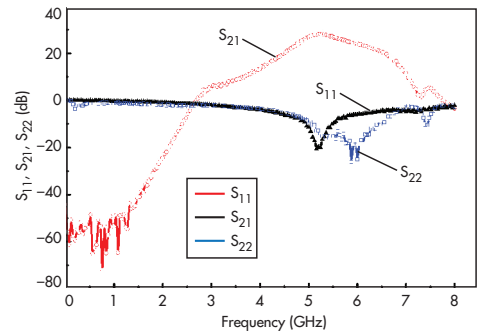
11. The photograph reveals the fabricated power amplifier module on the test board.

Designing WLAN PAs

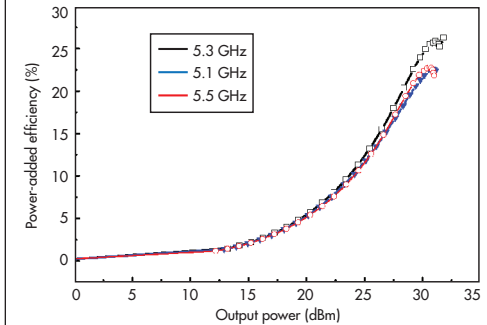
an inductor in the MMIC, a bond wire, and microstrip transmission lines on the laminate. The output matching network is formed by four bond wires and several surface-mount capacitors connected to inductors on the laminate.

Figure 12 presents the measured S_{11} , S_{21} , and S_{22} parameters for the PAM, measured with continuous-wave (CW) signals. The peak value for S_{21} is about 28.3 dB at 5.3 GHz. The small-signal gain for the PAM fluctuates within a 2-dB window across

12. The plots show measured S_{11} , S_{21} , and S_{22} for the PAM.



13. The plots show the measured dependence of the power gain on the output power of the PAM at 5.1, 5.5, and 5.7 GHz

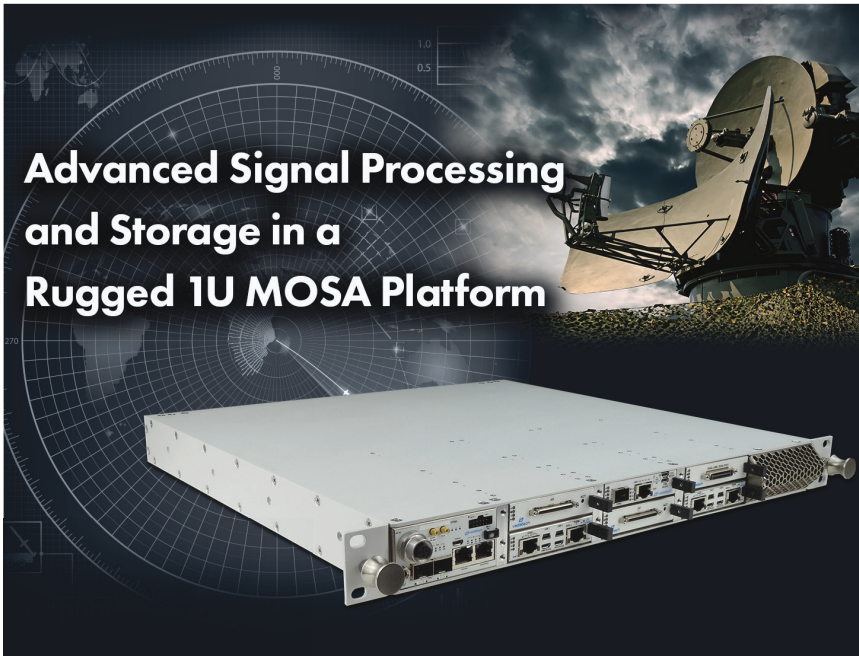


14. These plots reveal the measured dependence of PAE on the PAM's output power at 5.1, 5.5, and 5.7 GHz.

the frequency range, while S_{22} is less than -10 dB from 4.9 to 5.9 GHz.

Figure 13 depicts the dependence of the power gain on the output power of the PAM at +3.3-V dc bias at 5.1, 5.5, and 5.7 GHz. The saturated output power is greater than +31 dBm and the power gain is greater than 27 dB at all three frequencies. The saturated output power is greater than +30 dBm at 4.9, 5.7, and 5.9 GHz. The measured dependence of power added efficiency (PAE) on output power at 5.1, 5.3, and 5.5 GHz is plotted in Fig. 14, where PAE reaches 26.5% at 5.3 GHz. **MMW**

Note: For references, see the online version of this article at mwr.com.



ADC & DAC Modules

- Multi GSPS
- Up to 16-bit resolution
- Various channel densities
- FMC flexibility



FPGA Processing

- Broadest range of FPGAs
- Xilinx or Altera
- Full IP support



Storage Modules

- SAS-3 or SATA III, HDD or SSD
- RAID options to RAID 60
- Fixed or removable



Discover a powerful ruggedized open-standard platform. VadaTech's compact 1U form factor is modular, scalable, and configurable. Unrivaled SWaPc advantage for applications that require data acquisition, processing, networking, and storage.

VadaTech – Redefining performance density.



www.vadatech.com • info@vadatech.com • 702.896.3337